Journal of Nondestructive Evaluation (2022) 41:63
https://doi.org/10.1007/s10921-022-00895-w

Methodology for Mapping the Residual Stress Field in Serviced Rails Using L_{CR} Waves

Young-In Hwang[1] · Hyosung Lee[1,2] · Yong-Il Kim[1,3] · Ki-Bok Kim[1,2]

Received: 3 March 2022 / Accepted: 14 August 2022 / Published online: 8 September 2022

Abstract
Non-destructive stress measurement by ultrasonic testing is based on calculating the acoustoelastic modulus obtained from the relationship between material stress and sound wave velocity. A critically refracted longitudinal (L_{CR}) wave, which is a bulk longitudinal wave penetrating below and parallel to the surface below an effective depth, is most suitable for ultrasonic stress measurement tests because it exhibits a relatively large change in travel time in response to a change in stress. In particular, the residual stress distribution through the thickness of the subject can be calculated if transducers of different frequencies are applied because of the characteristic of propagation to different depths of penetration depending on the frequency. The main purpose of this study was to visualize the internal or residual stress distribution through the thickness of rails using L_{CR} waves. To this end, L_{CR} probes with different center frequencies were designed and manufactured, and the residual stress values of an unused railroad rail and two used railroad rails operated under different conditions were calculated. This was done using the ultrasonic signals received from each probe, of which the distributions were mapped. Through these mapping results, different residual stress values could be calculated according to the depth. The differences in residual stress generation and distribution according to the conditions surrounding the contact between train wheels and rails, and their characteristics, were visualized and analyzed. As a result, it could be concluded that the non-destructive evaluation technique using L_{CR} waves could detect differences in the residual stress of a rail, and thus can be used to measure the residual stress of the rail accurately.

Keywords Non-destructive evaluation (NDE) · Ultrasonic testing (UT) · Acoustoelastic effect · Critically refracted longitudinal (L_{CR}) wave · Residual stress mapping · Wheel-rail rolling contact · Railroad rail

1 Introduction

1.1 Railroad Rails

Rail transport is a means of transporting passengers and goods by wheeled vehicles running on railroads that connect cities to cities. It has been an efficient means of transportation, in terms of safety and economy, for a long time, and has contributed to the policy of suppressing the recent global warming problem with low carbon emission. In particular, since the opening of the first high-speed rails, the number of passengers using rail has increased, and the transportation volume of high-speed rail transport is rapidly increasing worldwide [1]. The global rail market showed an average growth of 3.6% from 2017 to 2019. Despite the decline of 8% in 2020 due to the Coronavirus disease-19 (COVID-19) pandemic, it is expected to show positive development in the mid- to long-term with an average annual growth rate of 2.3% until 2025 [2] (2.7% expected before the pandemic [3]).

On the other hand, the increase in traction and braking force due to the high speed of such railroad vehicles, and increase in the axle load to increase the efficiency of railroad

✉ Ki-Bok Kim
kimkibok@kriss.re.kr

1 Non-destructive Evaluation Team, Safety Measurement Institute, Korea Research Institute of Standards and Science, 267 Gajeong-ro, Yuseong-gu, 34113 Daejeon, Republic of Korea

2 Department of Measurement Engineering, University of Science and Technology, 217, Gajeong-ro, Yuseong-gu, 34113 Daejeon, Republic of Korea

3 Department of Nano Convergence Measurement, University of Science and Technology, 217, Gajeong-ro, Yuseong-gu, 34113 Daejeon, Republic of Korea

transportation, are aggravating the contact fatigue on the metal of the wheel-rail interface [4]. Because the speed and volume of rail transport is increasing, it is expected that the damage occurring at the interface between wheels and rails will accelerate. Therefore, research to reduce damage is urgently needed because a great deal of money is consumed in the maintenance and management of wheels and rails to ensure safe driving and riding comfort of the rail vehicles.

1.2 Rolling Contact Fatigue at the Wheel-Rail Interface

Railroad vehicles run by repeated rolling contact between wheels and rails. It is essential to understand the interaction caused by the rolling contact that occurs while a vehicle is traveling on rails. This is because one of the factors that greatly affects the safe operation and ride comfort of railway vehicles is the wheel-rail contact characteristic [5]. Friction caused by the wheel-rail rolling contact is an important factor that affects the braking and traction force of a vehicle. Too low friction causes problems with the vehicle's braking and traction [6]. On the other hand, wear or fatigue damage occurs at the wheel-rail contact surface due to repeated rolling contact [7]. Because the speed of railroad vehicles is increasing, the axle weight and traction force are also increasing, which causes more wheel and rail wear and fatigue damage. In addition, if damage to the wheel and rail is left unattended, fatigue cracks (or the like) may grow and cause breakage of the rail.

Fatigue damage caused by rolling contact at the wheel-rail contact surface due to the operation of the vehicle is caused by the simultaneous actions of physical and chemical mechanisms. The wheel-rail damage is affected by a wide variety of factors, such as contact characteristics according to wheel-rail shape, vehicle dynamic behavior, and vehicle track interaction. In addition, there is high potential for damage to increase rapidly due to increase in axle weights, increase in traffic volume, and change in the characteristics of wheel-rail materials [8]. Accordingly, the lifespan of the wheels and rails may be reduced at a faster rate than expected, and the rolling contact fatigue damage to the wheel and rail might cause a major accident, such as vehicle derailment, if not detected.

The contact characteristics between the wheel and the rail are greatly affected by their geometric shapes, which affects the maintenance of the rail. In particular, because the head of the rail that comes in direct contact with the wheel is greatly affected by the weight of the vehicle, traveling speed, and curvature of the vehicle, it should be considered first for compatibility with the vehicle [9].

According to the wheel shape and load conditions, the wheel contacts the rail surface asymmetrically, so uneven rolling contact fatigue appears in the rail head [10]. The geometric contact parameters of a wheel-rail interface include the rolling radii of the left and right wheels, the rolling radius difference, contact angle, contact angle difference, contact area, and ratio between the major and minor radii of the contact ellipse. Changes in these parameters change the position of the contact point between the wheel and rail [5, 7, 9]. Because the geometric shapes of the wheel and the rail greatly affect the characteristics of the contact between them, this change causes the load accumulated by different portions of the contact interface to be different.

1.3 Residual Stress Distribution in the Rail Head

Railroad rails are subjected to stresses generated through repeated interactions with train wheels. The load conditions generated on the rail by the wheels include the vertical load caused by the weight of the vehicle, the horizontal load generated when the vehicle passes through a curve, the tangential force generated during acceleration and deceleration of the vehicle, and the thermal load caused by brake heat in the case of a vehicle using such as tread braking [11, 12]. In addition, a dynamic load acts during the running of the vehicle. Among these loads, the vertical, horizontal, and tangential forces are transmitted to the rail by the contact between the wheel and the rail. The contact between the wheel and the rail occurs in the form of point contact or line contact with a small contact area [7]. Therefore, the contact stress generated by the wheel and the rail by the heavy railway vehicle exceeds the elastic limit. When the contact stress generated by the load exceeds the elastic limit, plastic deformation occurs at the contact surface of the wheel and rail, and residual stress is generated [11]. By measuring the residual stress due to frequent rolling contact, the characteristics of the load history of the contact surface can be determined. This stress also affects the occurrence of cracks; thus, it is an important factor affecting the strength and lifespan of a rail [13]. In other words, residual stress inevitably affects fatigue cracking, so measuring the residual stress accurately is the first step in evaluating service performance.

A curved railroad track is classified as a representative weakness of the track structure. Because the outer rail of a curve in the railroad track is subjected to strong lateral pressure and impact from the wheel flange to the gauge corner of the rail, substantial slip occurs along with rotation of the wheel, resulting in an imbalance in the internal stress distribution of the rail [14]. Therefore, the rail replacement cycle is typically faster for the curved portions of rail track than for straight track. However, the distribution of residual stresses in the head part of the rail is non-uniform even on a straight track, and depends on the wheel shape and load conditions.

The rail replacement cycle is generally set according to the accumulated tonnage, and in the case of curved parts, the wear limit of the amount of direct wear and uneven wear is set and the rail replaced before the limit is reached. The proportion of rail welding is increasing due to the use of long rails, and the rails on a straight general rail line has always exceeded the rail replacement standards, but there are many cases where they continue to be used without scientific evidence. In addition, because there are many standards that do not provide limit values for each train speed (including those in Korea [15]), there are many cases where rail lines are not suitable for the current high-speed situation. Therefore, to evaluate the safety of long-term rails exceeding the rail replacement standard, scientific analysis and a rationale for an effective rail-use limit considering the line conditions is required. Moreover, it is necessary to re-establish a standard for evaluation of the existing fatigue life. In other words, quantitative measurement of the residual stress distribution characteristics of rails is essential for determining the replacement cycle of rails and reducing track maintenance costs.

Accordingly, many studies have been conducted to measure the residual stress distributed in the wheels and rails. Kelleher et al. [16] measured residual stresses in slices of a new roller-straightened railroad rail and a worn ex-service rail using X-rays and the magnetic anisotropy and permeability system (MAPS). Lo et al. [14] measured residual principal stresses of a set of unused and used railroad rails of differing service times and loading histories with MAPS. Cal et al. [17] measured residual stresses on the surface of a rail joined by flash-butt welding using a hole-drilling method. Turan et al. measured residual stresses of rails that had the same casting number by cutting and X-ray diffraction methods [18]. Moreover, they measured residual stress in differently shaped rail specimens with a strain gauge and X-ray diffraction method, and examined microstructures in the specimens [19]. Jun et al. [20] obtained residual stresses at various positions on the rail and performed failure analyses on a fractured weld-repaired rail. Roy et al. [21] evaluated residual stresses of full-scale, cladded rails in the cladding layer, heat-affected zone (HAZ), and substrate using the neutron diffraction technique. Hwang et al. [22] measured stresses by applying tensile loads to unused rails and residual stresses remaining in used rails.

1.4 Ultrasonic Method of Residual Stress Measurement

Safety evaluation and judgment of usability through residual stress measurement on currently installed long-term rails must be performed non-destructively. Many non-destructive methods (involving such as ultrasonics, X-ray diffraction, neutron diffraction, magnetism, and electro-magnetism) have been developed and applied to measure stress [23]. Among them, the residual stress measurement using the ultrasonic method has an advantage different from the other techniques. Compared to the previously cited methods, the ultrasonic equipment is convenient and safe to use, quick to install, portable and inexpensive. Moreover, the measurement performance with ultrasonics provides a substantial depth of measurement and high spatial resolution. In addition, it can be applied regardless of the type of material or its thickness. Therefore, it is very suitable for on-site non-destructive inspection of previously installed structures, and is also suitable for measuring residual stress at a relatively deep position. In particular, because the stress measurement method using X-ray diffraction or Barkhausen noise can detect only the residual stress on the surface of an object, the ultrasonic method is suitable for inspection of subjects with different distributions of residual stresses according to depth, such as occurs with railroad rails.

Ultrasonic stress measurement technology is based on an acoustoelastic effect in which the velocity of propagating elastic waves in a solid depends on the applied or inherent stress [24]. Recently, many studies using critically refracted longitudinal (L_{CR}) waves (which are sensitive to changes in the internal stress field while less affected by the material texture [25]) have been conducted. Bray and Santos [26, 27] evaluated bending stress in plates and steel bars. They also measured residual stresses in aluminum and steel weld seams and determined the relaxation phenomenon of residual stress in the weld [28]. Sadeghi et al. [29] and Javadi et al. [30] measured through-thickness stress. Javadi et al. optimized the measurement of residual stresses generated by friction stir welding (FSW) of aluminum plates using the Taguchi method [31]. They also measured residual stress in stainless-steel welded plates with a finite element (FE) model and hole-drilling [32]. In later work, they evaluated welding residual stress of dissimilar joints using finite element welding simulation and compared immersion and contact ultrasonic methods [33]. They also [34–36] measured and evaluated the residual stresses of a stainless-steel welded plate and welded stainless-steel pipes of different thicknesses and at different wave frequencies. Xu et al. [37] tested residual stress in oil pipeline weld joints and many other mechanical components. Zhu et al. [38] estimated the residual stress of welded joints using the longitudinal critically refracted wave attenuation velocity (LCR-AV) method. Liu et al. [39] discussed the sensitivity of stress measurement accuracy to coupling conditions and temperature variation numerically and analytically. Yang et al. [40] measured the residual stresses of steel bars and investigated uncertain factors involved in measuring residual stress.

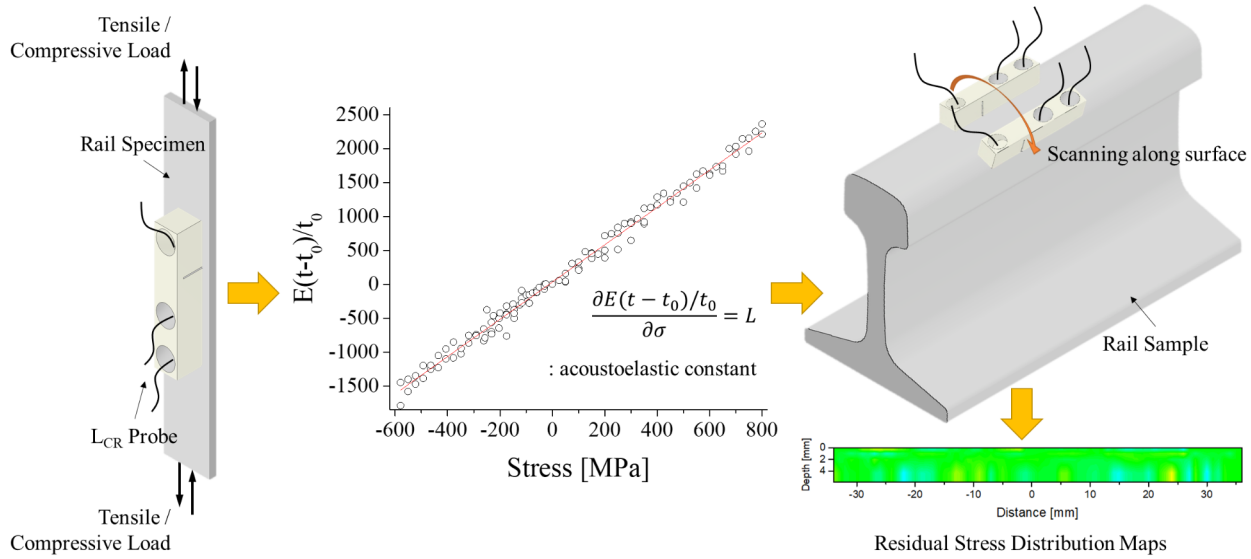

Fig. 1 Overview of the residual stress field mapping method using L_{CR} waves

Some studies have been conducted to measure residual stresses in rails specifically using L_{CR} waves. Egle and Bray [25] measured acoustoelastic constants for rail steel. Li et al. [41] utilized lifting scheme wavelet packet transform (LSWPT) as a denoising method on L_{CR} wave signals obtained by measuring the residual stress on the rail surface.

1.5 Objectives

The main purpose of this study was to understand the residual stress distribution according to the thickness of the rail using L_{CR} waves. To measure the residual stress in relation to depth, a number of probes with different center frequencies were fabricated. The residual stresses of unused rails and other railroad rails used under different service conditions were measured using ultrasonic signals received by individual probes. The residual stress distributions in each rail head were analyzed by mapping the calculated residual stress values from each probe. Figure 1 shows the overview of the residual stress field mapping method using L_{CR} waves.

2 Theory

2.1 Critically Refracted Longitudinal (L_{CR}) Wave Method

An L_{CR} wave is a longitudinal wave that is concentrated near the surface and travels parallel to the surface when the longitudinal wave is refracted at an incident angle greater than the first critical angle. Figure 2 shows schematic diagram of the L_{CR} wave propagation.

While this L_{CR} wave is sensitive to the stress field, it is less affected by the influence of the material structure. Accordingly, the L_{CR} wave method has an excellent advantage in non-destructive measurement of residual stress compared to other ultrasonic stress measurement methods. The stress measurement method using this wave is based on a linear relationship by which ultrasonic flight time varies according to the stress within the elastic limit. The relation between the flight time of L_{CR} waves and the stress is derived [25] as follows:

$$d\sigma = \frac{E(dV/V)}{L} = \frac{E}{Lt_0}(t - t_0 - dt_T) \tag{1}$$

where, $d\sigma$ is stress change, E is elastic modulus, V is the velocity of the longitudinal wave in a component, L is the acoustoelastic constant, t is flight time, t_0 is flight time when the wave traverses the path in the material under no applied stress, and dt_T is change in the flight time caused by temperature difference.

2.2 Mapping of the Residual Stress Field Using the L_{CR} Wave Method

The penetration depth of L_{CR} waves changes quantitatively as the center frequencies of the excitation and receiving transducers change [42]. The relationship between the penetration depth and frequency of L_{CR} waves satisfies the following empirical formula [43]:

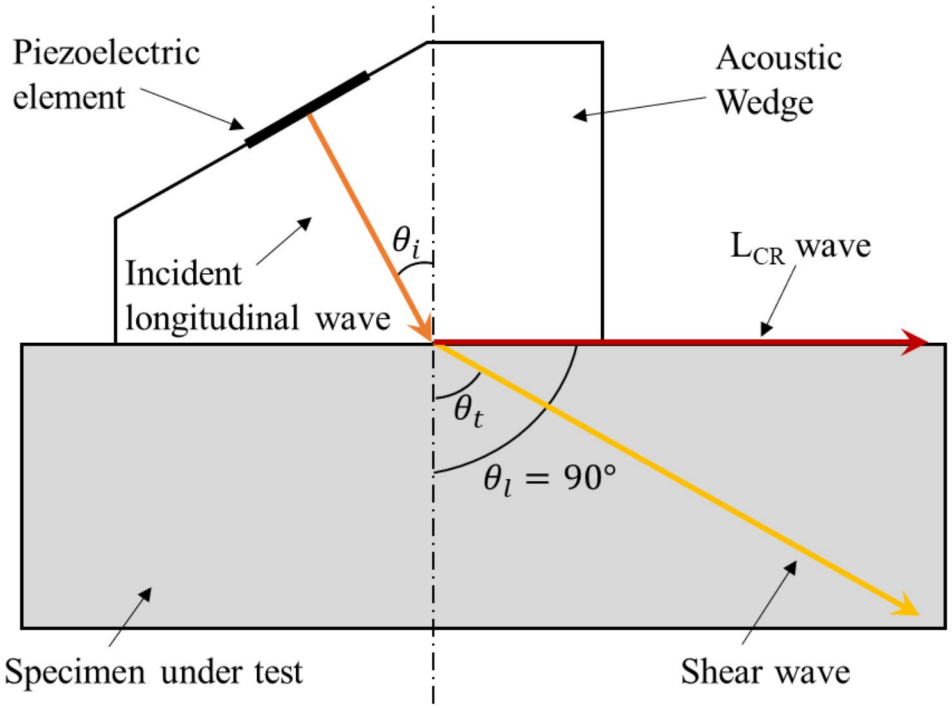

Fig. 2 Schematic diagram of the L_{CR} wave propagation

$$D = V \times f^{-0.96} \tag{2}$$

where, D is the penetration depth, and f is the center frequency of an ultrasonic transducer.

Residual stress at an optional depth can be calculated [43] using the following equation:

$$\sigma_{i-j} = \frac{\sigma_j D_j - \sigma_i D_i}{D_j - D_i} = \frac{\sigma_j f_j^{-0.96} - \sigma_i f_i^{-0.96}}{f_j^{-0.96} - f_i^{-0.96}} \tag{3}$$

3 Experimental Procedures

3.1 Sample Description

For the measurement of residual stresses using L_{CR} waves, three rail samples (one unused rail and two used rails) cut at different sites were used. The type of rail used to map the distribution of residual stress was 50 kgN [44], which is used for cargo and passenger transportation in Korea. All rail samples were part of straight rail tracks and were removed for replacement with new rails as they had been used beyond the cumulative passing tonnage specified in the regulations. Sample A was from the unused rail needed for comparison with the used rails. Sample B was a sample showing a relatively flat worn head surface, and Sample C was a sample with heavily worn gauge corners. Figure 3 shows the cross-section of the head of the rail samples used to map the residual stress distribution.

3.2 L_{CR} Probes

To describe the residual stress map in the rail, five L_{CR} probes with various center frequencies (0.5, 1, 2.25, 5, and 10 MHz) were fabricated. Each probe consisted of one transmitting transducer and one pair of receiving transducers for the same frequency, so that flight time could be calculated for the distance between the receiving transducers. In addition, two receivers were used to minimize the effect of environmental factors that could cause experimental errors such as temperature or coupling conditions. The L_{CR} probes were fabricated using $Pb(Mg_{1/3}Nb_{2/3})O_3$-$PbTiO_3$ (PMN-PT) elements, which exhibit better pulse echo signal amplitude over $Pb(Zr_xTi_{1-x})O_3$ (PZT) [45]. The inclination angle of the wedge (28.1°) is the first critical angle calculated according to Snell's law, and the wedges of the probes with frequencies from 0.5 to 2.25 MHz were fabricated using polymethyl methacrylate (PMMA). The wedges of the probes with frequencies of 5 MHz and 10 MHz were shorter and were made of Ultem polyetherimide. This is because the attenuation is severe and the amplitude of the received signal is low when using relatively high frequencies. To make the wedges shorter, 0.25-inch piezoelectric elements were used for these probes, compared to the 0.5-inch piezoelectric element diameters of the other transducers. The newly fabricated probes are shown in Fig. 4.

Table 1 shows each penetration depth according to frequency, as calculated using Eq. 3.

(a) (b) (c)

Fig. 3 Cross-section photograph of the head part of the rail samples: (a) Sample A, (b) Sample B, and (c) Sample C

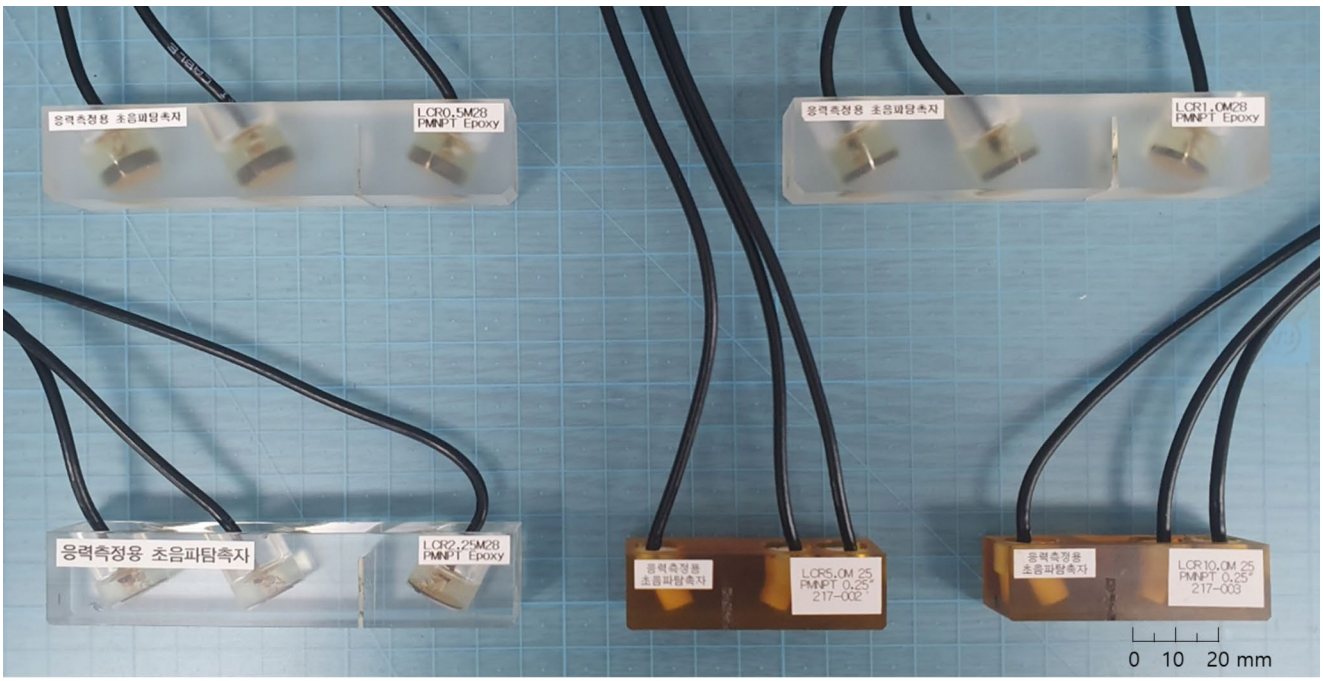

Fig. 4 Photograph of the five L_{CR} probes

Table 1 Calculated penetration depths for each L_{CR} wave frequency

Frequency [MHz]	0.5	1	2.25	5	10
Penetration depth [mm]	11.477	5.900	2.709	1.258	0.647

3.3 Measurement Devices

Each fabricated L_{CR} probe was connected to a pulser/receiver (APR-8035, AcouLab, Korea) and attached to a rail specimen. Ultrasonic signals were acquired in each specific frequency range by adjusting high- and low-pass filters according to the center frequencies of the connected ultrasonic probes. A workstation controlled the pulser/receiver to excite ultrasound at the transmitter and to acquire ultrasonic waves at the receivers. Excited longitudinal waves were transmitted through the wedge of the probe and the L_{CR} waves propagated along the surface of the rail sample were received by each receiver and displayed on an oscilloscope (WaveRunner 640Zi, Teledyne LeCroy, USA). The experimental setup for measuring residual stresses using L_{CR} waves is shown in Fig. 5.

3.4 Residual Stress Mapping

To map a residual stress field that is non-uniformly distributed according to the characteristics of the direction in which the vehicle's load is applied and the shape of the wheel, ultrasonic signals were acquired by changing the position of the probe at intervals of 1 mm in the direction perpendicular to the length direction of the rail. As shown in Fig. 6., ultrasound signals were acquired by scanning the same area using five developed probes, and residual stresses

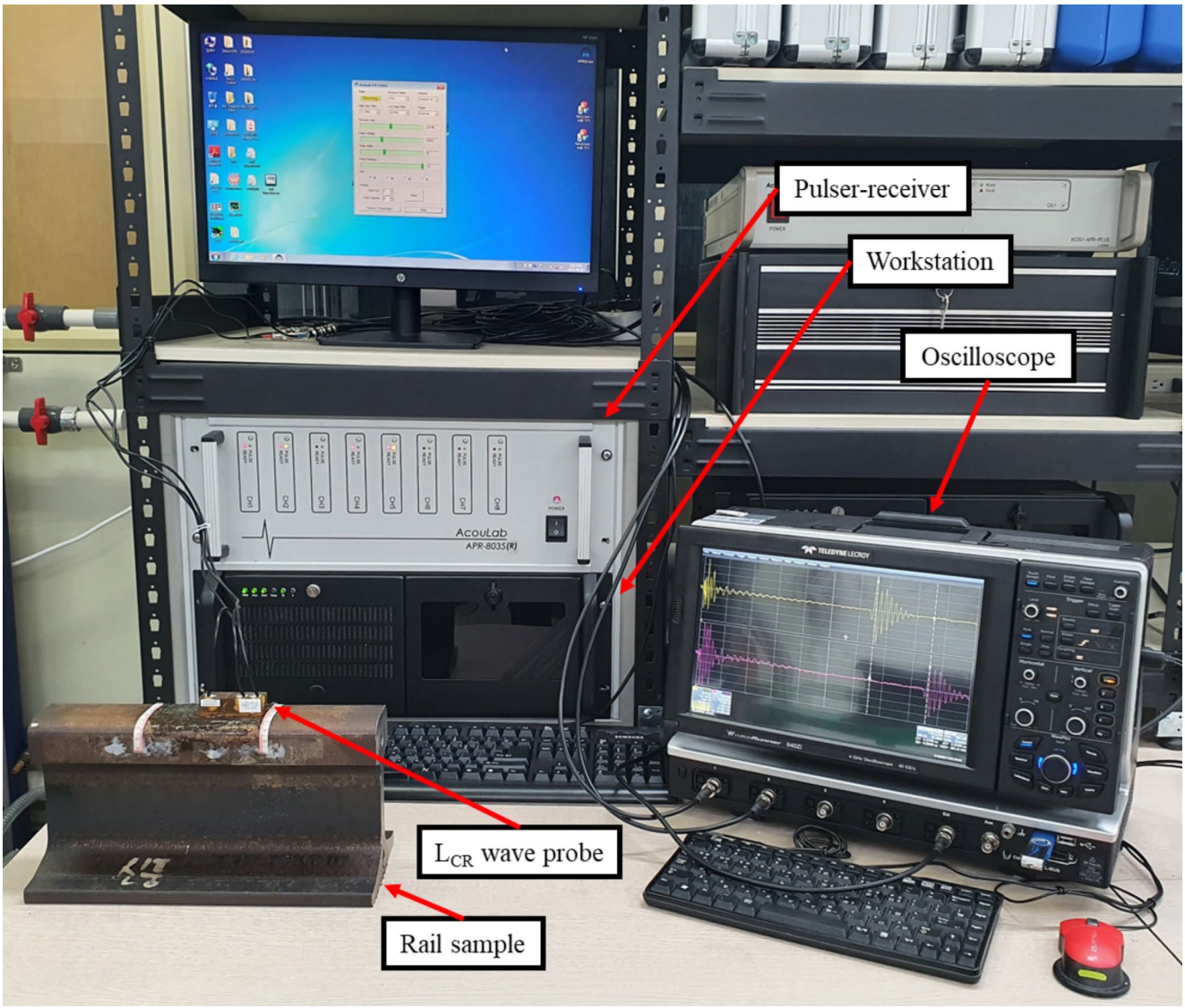

Fig. 5 Photograph of the experimental setup for measuring residual stresses using L_{CR} waves

at each depth of penetration for all scanned positions for field mapping were measured.

When the probe was attached to a surface with a relatively high curvature or an unspecified surface due to wear, the ultrasonic signal could not be normally received because the wedge bottom and the rail surface did not adhere properly, and there was a possibility that an experimental error might occur. As a countermeasure for this case, a pad-typed elastomer (Aqualene Elastomer Couplant, Olympus, Japan) was attached between the bottom of the probe wedge and the top of the rail. This aqualene dry couplant has almost the same acoustic impedance as water and has a low damping coefficient. And, it has strong elasticity and flexibility, so it can be easily deformed according to the shape of the contact surface by lightly pressing the probe. Figure 7 is shown to supplement the explanation of the application of different couplants according to the curvature of the surface of the rail head. The ultrasonic signals obtained this way were used to calculate residual stress values for each position using the acoustoelastic modulus of the rail presented in an existing research paper [46].

4 Results and Discussion

The residual stress values calculated for each position are shown through the results of linear scanning on the three rail samples using each probe. The results in the graphs (colored lines) indicate the results for the center frequency of each probe, for each rail sample, as shown in Fig. 8. Here, the x-axis does not mean the horizontal distance, but the distance from the center of the rail to the contact point of

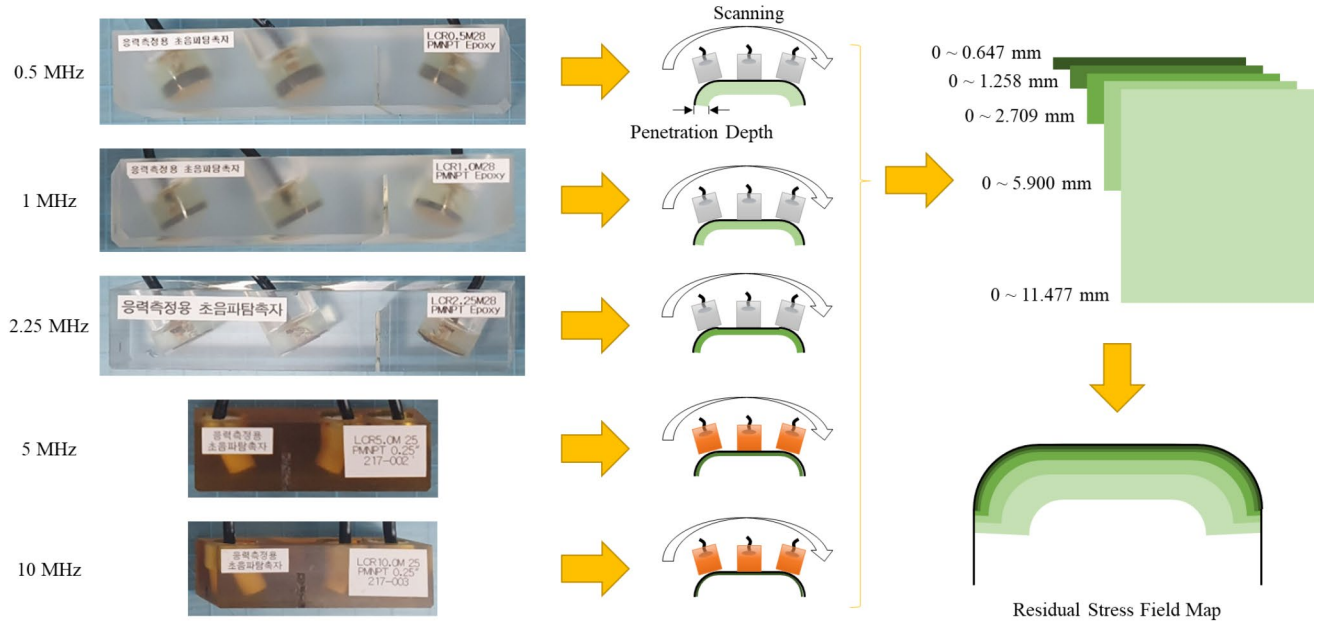

Fig. 6 Scanning using five L_{CR} probes with different frequency for residual stress mapping

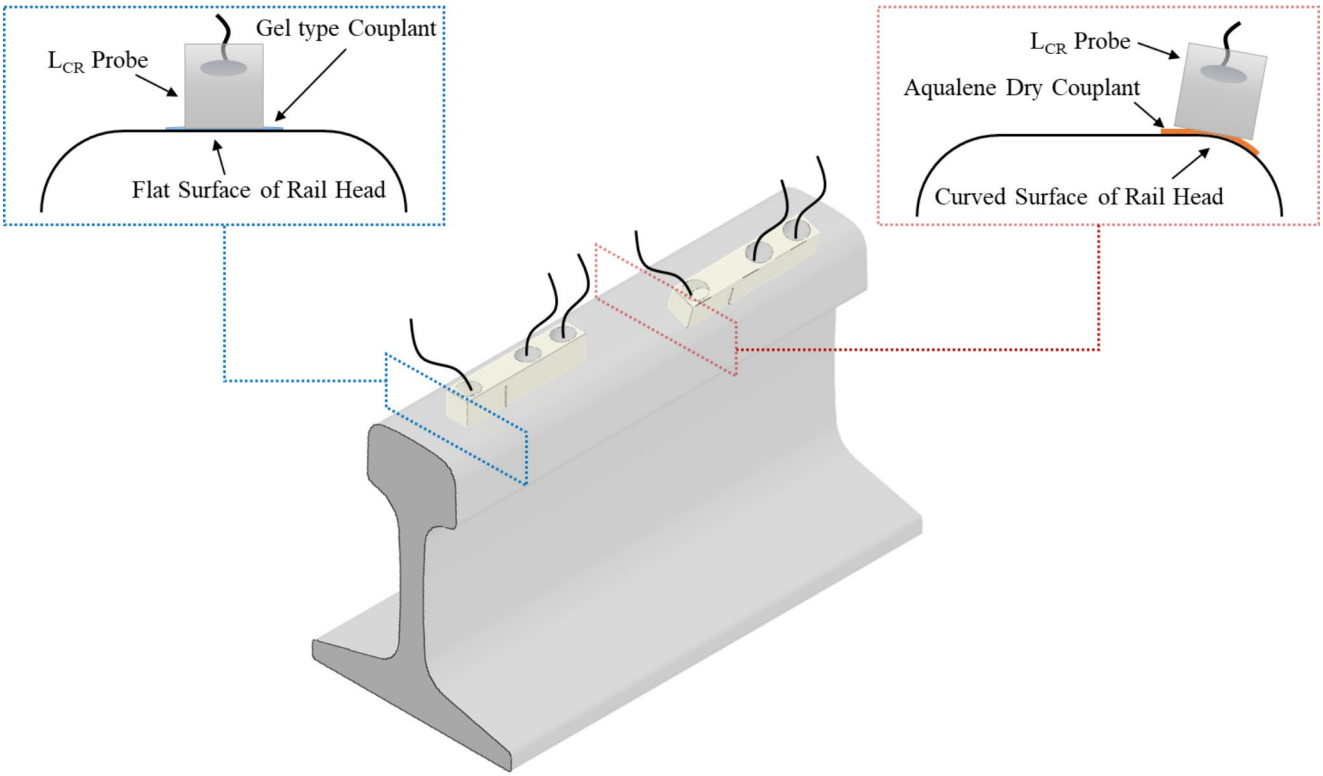

Fig. 7 Schematic diagram of scanning using the L_{CR} wave probe with different types of couplants applied depending on the curvature of the rail head

the probe in contact with the rail head surface. And, negative values on the y-axis mean compressive residual stress, and positive values on the same axis mean tensile residual stress.

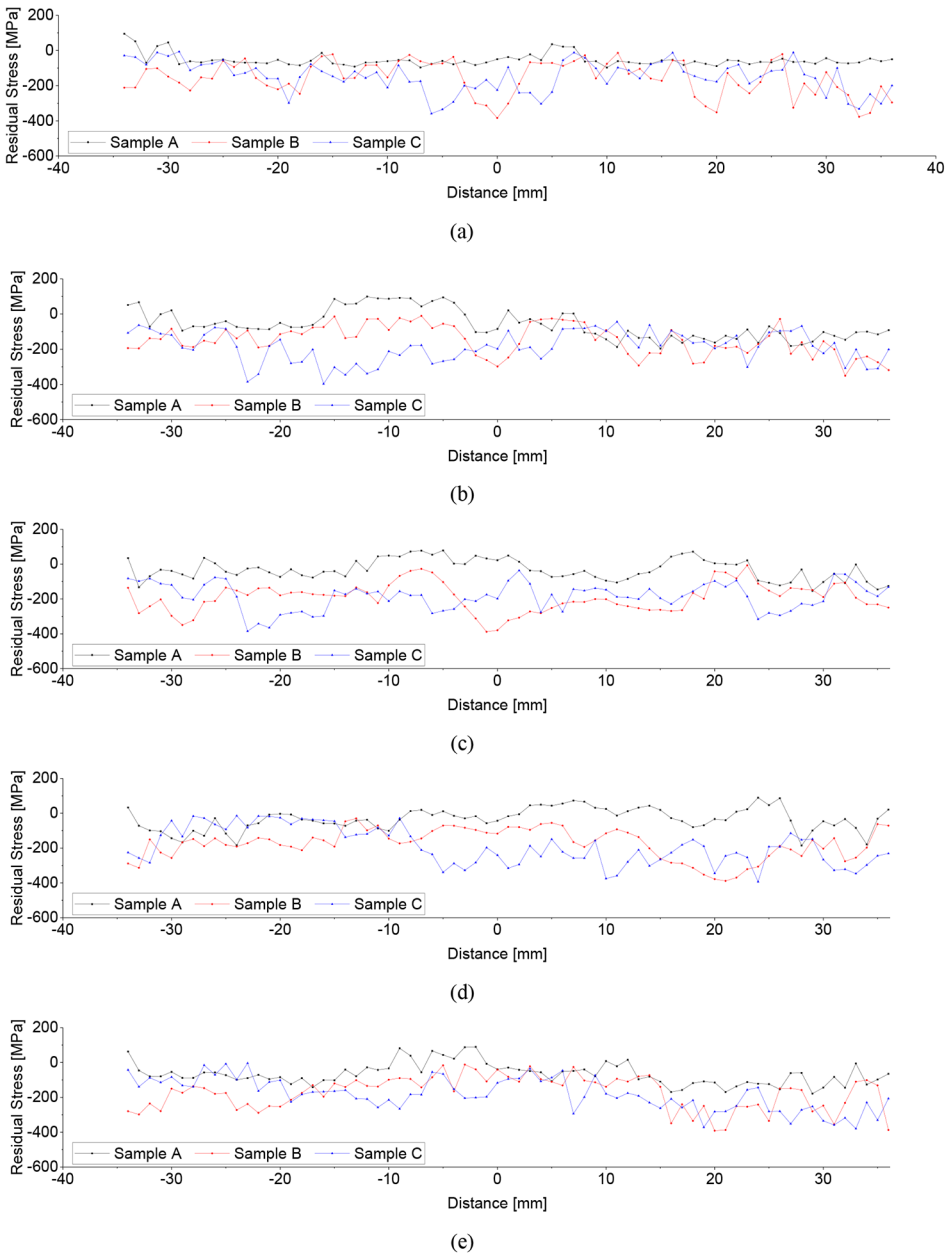

Fig. 8 Results from calculating residual stress values for three rail samples obtained through linear scanning using five probes with different center frequencies: (a) 0.5 MHz, (b) 1 MHz, (c) 2.25 MHz, (d) 5 MHz, and (e) 10 MHz

Regardless of the center frequency, the compressive residual stress was found in the serviced rails rather than the unused rail (Sample A). On the other hand, residual stress values measured with low-frequency (0.5 MHz) or high-frequency (10 MHz) L_{CR} waves tended to have noisy signals or relatively poor resolution.

Due to the difference in the penetration depth of the L_{CR} waves according to frequency, the waves move shallower as the measurement frequency increases, so the residual stress in the deeper layer can be confirmed as a relatively low frequency wave. Therefore, residual stress values according to depth were calculated by substituting the data in Fig. 8 into Eq. (3), and the results are shown in Fig. 9.

As a result of visualizing the residual stress values according to depth, unlike with the classification of results according to the center frequency, it was observed that the compressive residual stress values were higher at shallow depths (0–2.709 mm).

As illustrated in Fig. 6, using the results for the residual stress distribution along the thickness direction obtained from Fig. 9, the stress gradient around the surface of the head parts in the transverse cross-sections of the rail samples can be visualized as shown in Fig. 10.

As a result of examining the residual stress distribution of the rail shown in Fig. 10, it was visualized from the map of the used rail samples that the compressive residual

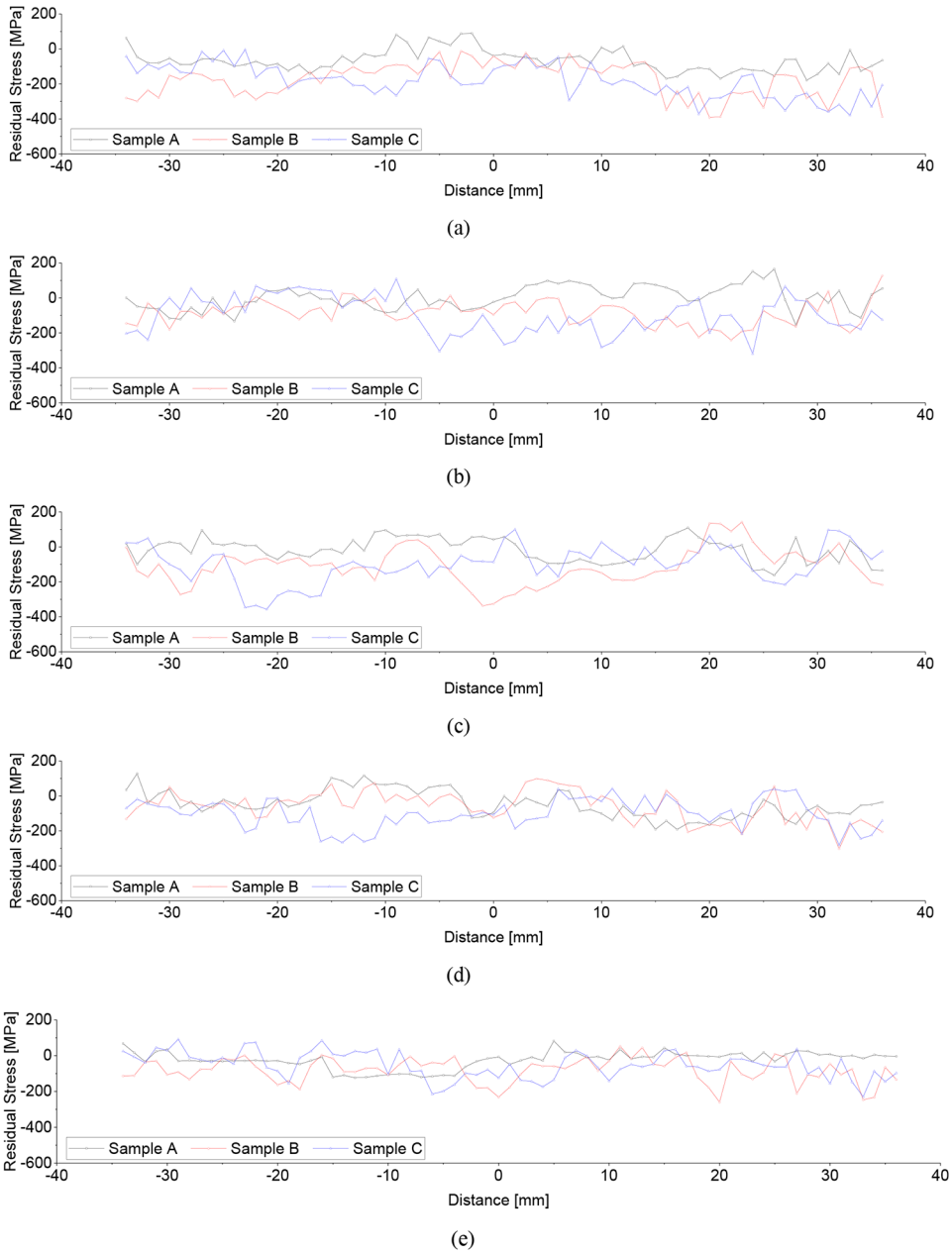

Fig. 9 Results from calculating residual stress values for each layer in depth: (a) 0.000–0.647 mm, (b) 0.647–1.258 mm, (c) 1.258–2.709 mm, (d) 2.709–5.900 mm and (e) 5.900–11.477 mm

stresses were large in the area of the rail surface where wear occurred. That is, Fig. 10 shows that the residual stress value of the rail and the pattern of its distribution can change when the traffic load is accumulated. In the case of Sample 3, it was possible to predict that the residual stress was biased toward the gauge corner (on the right side of the image) because of severe, visually apparent uneven wear, so the mapping result came out as expected. However, it was quantitatively confirmed that even in the case of Sample 2, which was confirmed to be uniformly worn when checked with the naked eye, higher residual stress was inherent in the portion where the wheel was in direct contact.

However, when the curvature of the rail surface was changed, it was confirmed that the error of the results increased due to a difference in the degree of adhesion between the L_{CR} probe and the surface of the sample.

5 Conclusion

A study was conducted to visualize the stress distribution according to depth by measuring the residual stress of rails based on the ultrasonic acoustoelastic effect. The residual stress was measured using L_{CR} waves, which are the most sensitive longitudinal wave, and the residual stress values

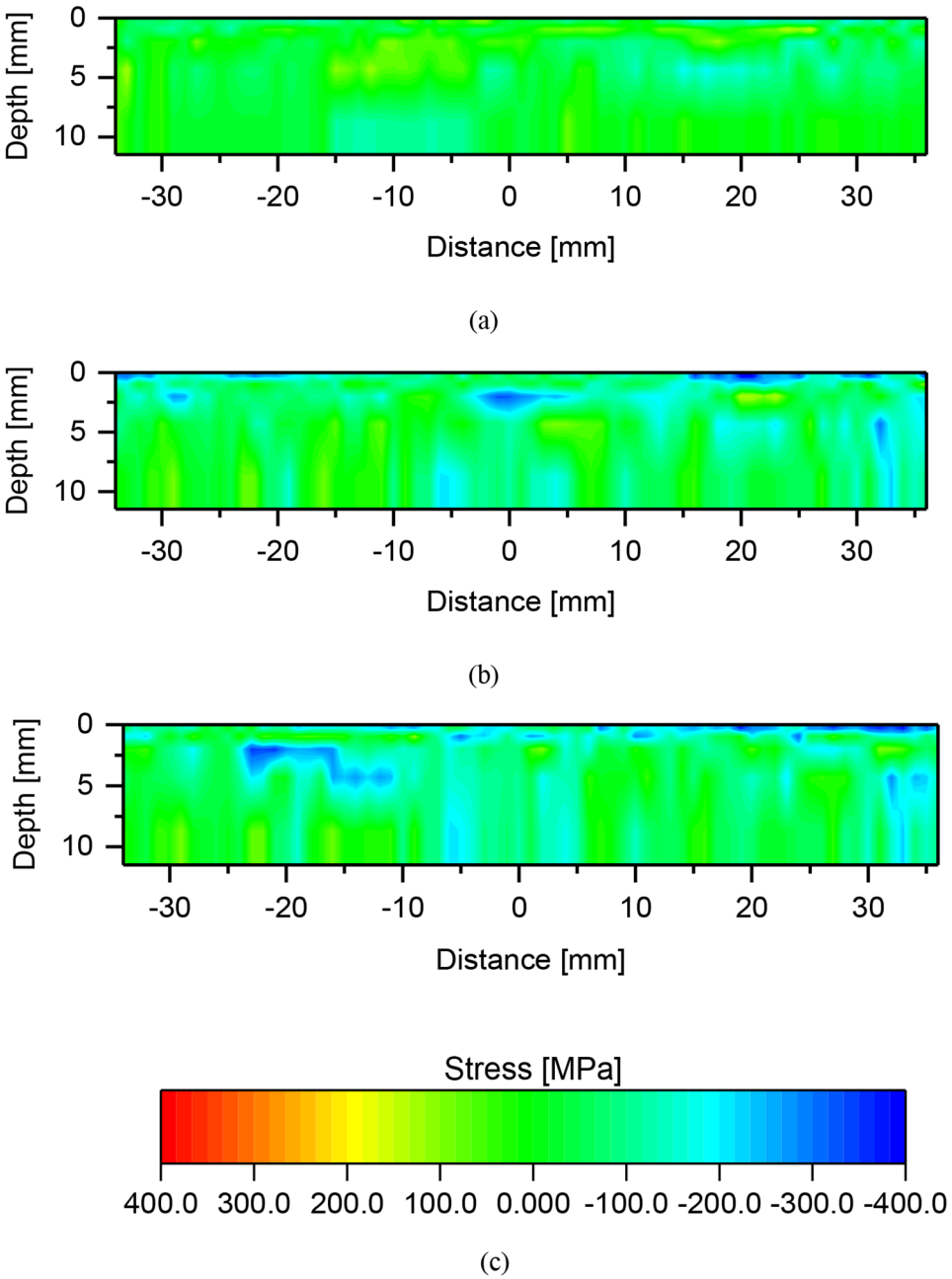

Fig. 10 Residual stress distribution maps for (a) Sample A, (b) Sample B, and (c) Sample C

inside the rail head were calculated by scanning the head of three rail samples subjected to different conditions, using L_{CR} probes with five center frequencies (0.5, 1, 2.25 MHz and 5, 10 MHz) in two sizes. Through this study, it was confirmed that the measured residual stress values depicted in the map were quantitatively calculated in proportion to the degree of partial wear that could be observed with the naked eye.

On the other hand, according to the methodology presented in this paper, the residual stress measurement apparatus using L_{CR} waves could be miniaturized, so it could be applied to real-time stress measurement at sites where rails are installed by constructing a portable system. In particular, when a rail is cut, the residual principal stress in the direction parallel to the cut surface is not relieved very much, but the principal stress along the longitudinal direction of the rail is relaxed. For this reason, it is very important to measure the stress of installed rails to measure the actual residual stress value. Therefore, this approach can be proposed as an alternative solution to overcome the limitations of measuring the residual stress of a rail using the Barkhausen noise method or X-ray diffraction method, which is too restrictive to make the equipment portable.

Funding This research was supported by a "development of safety measurement technology for infrastructure industry" grant funded by the Korea Research Institute of Standards and Science (KRISS-2022-GP2022-0010).

Declarations

Competing Interests The authors have no financial or proprietary interests in any material discussed in this article.

References

1. The perpetual growth of high-speed rail development:. Available online: (2021). https://www.globalrailroadreview.com/article/112553/perpetual-growth-high-speed-rail/ (accessed on 09
2. Berger, R.U.N.I.F.E. World Rail Market Study - Forecast 2020 to 2025. (2020)
3. Berger, R.U.N.I.F.E. World Rail Market Study - Forecast 2018 to 2023. (2018)
4. Mutton, P.J., Epp, C.J., Dudek, J.: Rolling contact fatigue in railway wheels under high axle loads. wear. 144(1–2), 139–152 (1991)
5. Zhang, H., Ran, X., Wang, X., Lin, F., Jiang, Q. Coupling Effects of Yaw Damper and Wheel-Rail Contact on Ride Quality of Railway Vehicle. *Shock and Vibration*, 2021. (2021)
6. Arias-Cuevas, O., Li, Z., Lewis, R.: Investigating the lubricity and electrical insulation caused by sanding in dry wheel–rail contacts. Tribol. Lett. 37(3), 623–635 (2010)
7. Soleimani, H., Moavenian, M.: Tribological aspects of wheel–rail contact: a review of wear mechanisms and effective factors on rolling contact fatigue. Urban Rail Transit. 3(4), 227–237 (2017)
8. Zerbst, U., Lundén, R., Edel, K.O., Smith, R.A.: Introduction to the damage tolerance behaviour of railway rails–a review. Eng. Fract. Mech. 76(17), 2563–2601 (2009)
9. Popović, Z., Lazarević, L., Brajović, L., Vilotijević, M.: The importance of rail inspections in the urban area-aspect of head checking rail defects. Procedia Eng. 117, 596–608 (2015)
10. Jun, T.S., Hofmann, F., Belnoue, J., Song, X., Hofmann, M., Korsunsky, A.M.: Triaxial residual strains in a railway rail measured by neutron diffraction. J. Strain Anal. Eng. Des. 44(7), 563–568 (2009)
11. Orringer, O., Orkisz, J., Swiderski, Z. (eds.): Residual Stress in Rails: Effects on Rail Integrity and Railroad Economics Volume II: Theoretical and Numerical Analyses, vol. 12. Springer (2017)
12. Johns, T.G., Davies, K.B., McConnell, D.P. *Introduction to stresses in rails: stresses in midrail regions* (No. 694). (1978)
13. Ekberg, A., Åkesson, B., Kabo, E.: Wheel/rail rolling contact fatigue–Probe, predict, prevent. Wear. 314(1–2), 2–12 (2014)
14. Lo, K.H., Mummery, P., Buttle, D.J.: Characterisation of residual principal stresses and their implications on failure of railway rails. Eng. Fail. Anal. 17(6), 1273–1284 (2010)
15. Authority, Korea Rail Network. "Guidelines of track maintenance." (2020)
16. Kelleher, J., Prime, M.B., Buttle, D., Mummery, P.M., Webster, P.J., Shackleton, J., Withers, P.J.: The measurement of residual stress in railway rails by diffraction and other methods. J. Neutron Res. 11(4), 187–193 (2003)
17. Cal, Z., Nawafune, M., Ma, N., Qu, Y., Cao, B., Murakawa, H.: Residual stresses in flash butt welded rail. Trans. JWRI. 40(1), 79–87 (2011)
18. Turan, M.E., OZCELIK, S., ZENGIN, H., Tozlu, A.H.L.A.T.C.I.,H.T.U.R.E.N.Y., I., & SUN, Y. Residual stress measurement in rails by destructive and non destructive method. *Metal* 2015, 1–6. (2015)
19. Turan, M.E., Aydin, F., Sun, Y., Cetin, M.: Residual stress measurement by strain gauge and X-ray diffraction method in different shaped rails. Eng. Fail. Anal. 96, 525–529 (2019)
20. Jun, H.K., Seo, J.W., Jeon, I.S., Lee, S.H., Chang, Y.S.: Fracture and fatigue crack growth analyses on a weld-repaired railway rail. Eng. Fail. Anal. 59, 478–492 (2016)
21. Roy, T., Paradowska, A., Abrahams, R., Law, M., Mutton, P., Soodi, M., Yan, W.: Residual stress in laser cladded heavy-haul rails investigated by neutron diffraction. J. Mater. Process. Technol. 278, 116511 (2020)
22. Hwang, Y.I., Kim, Y.I., Seo, D.C., Seo, M.K., Lee, W.S., Kwon, S., Kim, K.B.: Experimental Consideration of Conditions for Measuring Residual Stresses of Rails Using Magnetic Barkhausen Noise Method. Materials. 14(18), 5374 (2021)
23. Chakrabarti, R., Biswas, P., Saha, S.C.: A review on welding residual stress measurement by hole drilling technique and its importance. J. Weld. Join. 36(4), 75–82 (2018)
24. Kudryavtsev, Y., Kleiman, J., Gushcha, O., Smilenko, V., Brodovy, V. Ultrasonic technique and device for residual stress measurement. In *X International Congress and Exposition on Experimental and Applied Mechanics. Costa Mesa, California USA* (pp. 1–7). (2004), June
25. Egle, D.M., Bray, D.E.: Measurement of acoustoelastic and third-order elastic constants for rail steel. J. Acoust. Soc. Am. 60(3), 741–744 (1976)
26. Bray, D.E., Tang, W.: Subsurface stress evaluation in steel plates and bars using the LCR ultrasonic wave. Nucl. Eng. Des. 207(2), 231–240 (2001)
27. dos Santos, A.A. Jr., Bray, D.E.: Comparison of acoustoelastic methods to evaluate stresses in steel plates and bars. J Press. Vessel Technol. 124(3), 354–358 (2002)
28. Andrino, M.H., dos Santos Jr., A.A., Bray, D.E., Trevisan, R.E. Stress relaxation in aluminum welding using ultrasonic method. In *ASME Pressure Vessels and Piping Conference* (Vol. 42835, pp. 157–165). (2007), January
29. Sadeghi, S., Najafabadi, M.A., Javadi, Y., Mohammadisefat, M.: Using ultrasonic waves and finite element method to evaluate through-thickness residual stresses distribution in the friction stir welding of aluminum plates. Mater. Design. 52, 870–880 (2013). (1980–2015
30. Javadi, Y., Akhlaghi, M., Najafabadi, M.A.: Using finite element and ultrasonic method to evaluate welding longitudinal residual stress through the thickness in austenitic stainless steel plates. Mater. Design. 45, 628–642 (2013)
31. Javadi, Y., Sadeghi, S., Najafabadi, M.A.: Taguchi optimization and ultrasonic measurement of residual stresses in the friction stir welding. Mater. Design. 55, 27–34 (2014)
32. Javadi, Y., Akhlaghi, M., Najafabadi, M.A.: Nondestructive evaluation of welding residual stresses in austenitic stainless steel plates. Res. Nondestr. Eval. 25(1), 30–43 (2014)
33. Javadi, Y., Najafabadi, M.A.: Comparison between contact and immersion ultrasonic method to evaluate welding residual stresses of dissimilar joints. Mater. Design. 47, 473–482 (2013)
34. Javadi, Y., Plevris, V., Najafabadi, M.A.: Using L_{CR} ultrasonic method to evaluate residual stress in dissimilar welded pipes. Int. J. Innov. Manage. Technol. 4(1), 170–174 (2013)
35. Javadi, Y., Pirzaman, H.S., Raeisi, M.H., Najafabadi, M.A.: Ultrasonic inspection of a welded stainless steel pipe to evaluate residual stresses through thickness. Mater. Design. 49, 591–601 (2013)
36. Javadi, Y., Hloch, S. Employing the L_{CR} waves to measure longitudinal residual stresses in different depths of a stainless steel welded plate. *Advances in Materials Science and Engineering*, 2013. (2013)

37. Xu, C., Song, W., Pan, Q., Li, H., Liu, S.: Nondestructive testing residual stress using ultrasonic critical refracted longitudinal wave. Phys. Procedia. 70, 594–598 (2015)
38. Zhu, Q., Chen, J., Gou, G., Chen, H., Li, P.: Ameliorated longitudinal critically refracted—Attenuation velocity method for welding residual stress measurement. J. Mater. Process. Technol. 246, 267–275 (2017)
39. Liu, H., Li, Y., Li, T., Zhang, X., Liu, Y., Liu, K., Wang, Y.: Influence factors analysis and accuracy improvement for stress measurement using ultrasonic longitudinal critically refracted (LCR) wave. Appl. Acoust. 141, 178–187 (2018)
40. Yang, S., Wang, M., Yang, L.: Investigation of uncertain factors on measuring residual stress with critically refracted longitudinal waves. Appl. Sci. 9(3), 485 (2019)
41. Li, P., Xu, C., Pan, Q., Lu, Y., Li, S.: Denoising of LCR Wave Signal of Residual Stress for Rail Surface Based on Lifting Scheme Wavelet Packet Transform. Coatings. 11(5), 496 (2021)
42. Song, W.T., Pan, Q.X., Xu, C.G., Li, X., Jin, X., Li, H.X., Liu, S.: Residual stress nondestructive testing for pipe component based on ultrasonic method. In: 2014 IEEE Far East Forum on Nondestructive Evaluation/Testing, pp. 163–167. IEEE (2014, June)
43. Song, W., Xu, C., Pan, Q., Song, J.: Nondestructive testing and characterization of residual stress field using an ultrasonic method. Chin. J. Mech. Eng. 29(2), 365–371 (2016)
44. Korean Railway, Standards, KRS TR 0001–15(R), Rail, Railway Technology Review Committee (2006)
45. Kim, K.B., Hsu, D.K., Ahn, B., Kim, Y.G., Barnard, D.J.: Fabrication and comparison of PMN-PT single crystal, PZT and PZT-based 1–3 composite ultrasonic transducers for NDE applications. Ultrasonics. 50(8), 790–797 (2010)
46. Hwang, Y.I., Kim, G., Kim, Y.I., Park, J.H., Choi, M.Y., Kim, K.B.: Experimental Measurement of Residual Stress Distribution in Rail Specimens Using Ultrasonic L_{CR} Waves. Appl. Sci. 11(19), 9306 (2021)